Available online at website: https://journal.bcrec.id/index.php/bcrec

Bulletin of Chemical Reaction Engineering & Catalysis, 20 (4) 2025, 683-693

Original Research Article

Enhanced Adsorption of Brilliant Green Dye Using Barium Ferrite/Graphene Oxide Nanocomposites

Usama A. Saed[1], Alaa H. Ali[2], Ammar A. Saoud[1], Zeyad Zeitoun[3,4,*]

[1]Chemical Engineering Department, College of Engineering, Al-Nahrain University, Baghdad, Iraq.
[2]Scientific Research Commission, Ministry of Higher Education and Scientific Research, Baghdad, Iraq.
[3]Department of Engineering and Computer Science, McNeese State University, Lake Charles 70605, LA, United States.
[4]Chemical Engineering Department, Faculty of Engineering, Alexandria University, Alexandria 21544, Egypt.

Received: 25th July 2025; Revised: 5th October 2025; Accepted: 7th October 2025
Available online: 12th October 2025; Published regularly: December 2025

Abstract

This study presents the synthesis and characterization of barium ferrite/graphene oxide (BaFeO/GO) nanocomposites for the adsorption of brilliant green dye (BGD) from aqueous solutions. BaFeO/GO nanocomposites were fabricated via a co-precipitation method with varying GO content (10-30 wt%), and characterized using Fourier Transform Infra rEd (FTIR), X-Ray Diffraction (XRD), Scanning Electron Microscope (SEM), Field-Emission Scanning Electron Microscopy (FESEM), Transmission Electron Microscope (TEM), Brunauer, Emmett, and Teller (BET), and Vibrating Sample Magnetometer (VSM) techniques. The incorporation of GO enhanced the surface area, reduced BaFeO nanoparticle agglomeration, and introduced additional oxygen-containing functional groups, significantly improving the adsorption performance. Batch adsorption experiments were conducted to evaluate the effects of pH, contact time, adsorbent dose, and initial dye concentration. The maximum dye removal efficiency reached 98.9% with the BaFeO/30%GO composite. Kinetic studies showed excellent agreement with the pseudo-second-order model, while adsorption isotherm analysis indicated that the Langmuir model best fit the equilibrium data, suggesting monolayer adsorption. These results demonstrate the potential of BaFeO/GO nanocomposites as efficient, magnetically separable adsorbents for the removal of cationic dyes from wastewater.

Keywords: Wastewater Treatment; Adsorption; Graphene Oxide Nanocomposites; Brilliant Green Dye

How to Cite: Saed, U.A., Ali, A.H., Saoud, A.A., Zeitoun, Z. (2025). Enhanced Adsorption of Brilliant Green Dye Using Barium Ferrite/Graphene Oxide Nanocomposites. *Bulletin of Chemical Reaction Engineering & Catalysis*, 20 (4), 683-693. (doi: 10.9767/bcrec.20453)

Permalink/DOI: https://doi.org/10.9767/bcrec.20453

1. Introduction

Dyes - those vibrant compounds that bring color to our everyday lives - are more than just pigments. A dye is an aromatic and ionizing substance that forms a chemical bond with the material it colors. These substances, often called coloring agents, vary widely in their chemical makeup [1]. Based on the chromophores (the part of the molecule responsible for color), dyes are generally classified into five major groups: anthraquinone, azo, indigoid, phthalocyanine, and arylmethane. Dyes play a crucial role in numerous industries, from paint and plastics to paper, cosmetics, food, and furniture [2]. However, the textile industry nowadays stands out as the largest consumer of dyes and pigments and has exploded in scale. For instance, the total textile dye consumption is greater than 107 kg per year worldwide with roughly 106 kg per year of dyes discharged into water streams killing more than three million people, mainly infants, who get water for drinking and irrigation [3]. Moreover,

* Corresponding Author.
Email: zzeitoun@mcneese.edu (Z. Zeitoun)

millions of tons of cloth are produced each year, and it is now one of the most important industries in the world, employing more than a million people. But this rapid growth carries a steep environmental cost largely owing to the huge volumes of wastewater it produces, Water is a key force behind textile production – it is used copiously in processes like dyeing, washing, and finishing. This wastewater is frequently filled with a hodgepodge of dangerous toxins that can create significant environmental and public health hazards. In addition, the world's fresh water is rapidly becoming scarcer from both large scale industrial pollution, and the continued impacts of climate change. To address this, the textile industries is now faced with a growing issue of how to develop effective practices for treating dye containing effluent, so that discharge does not further endanger the environment and the quality of the receiving water bodies is protected [4].

Currently, the treatment of dye pollutants, especially brilliant green dye, in textile wastewater has been receiving much attention. A variety of treatment methods have been investigated, from chemical precipitation, chemical oxidation, coagulation/flocculation, ion exchange, biological treatment, electrolysis, membrane technology to adsorption. However, all of these techniques have certain drawbacks that prevent their routine use. For example, chemical precipitation tends to produce relatively large volumes of sludge, driving difficulties in managing and disposing of such large quantities requiring greater cost of operation. The chemical oxidation entails unidentified intermediate products, has a relatively short half-life when the oxidant is ozone, or may even generate sludge with an emission of volatile organic compounds and aromatic amines [5]. Since coagulation and flocculation use coagulant and flocculant repeatedly, the demand for a non-reusable chemical is increasing, resulting in secondary pollution and increased costs. Ion exchange procedures involve bulky column configurations and are strongly pH-dependent of the eluent [6]. In addition to this, they tend to be ineffective at degrading some pollutants e.g. dyes and pharmaceuticals. Biological processes require the cultivation and nurture of microorganisms, need pre-treatment with physicochemical methods, and are in general slow. Furthermore, the poor biodegradability of dye molecules leads to low decolorization efficiency as well as sludge bulking and foaming problems [7]. Although, electrolysis is efficient, the cost of the equipment and maintenance is high and become expensive at the beginning. Anode passivation, sludge formation on electrodes and bubble size-related inefficiency are the main factors to prevent its continuous operation [8]. On the other hand, membrane processes give rise to high energy demand, high maintenance and expensive equipment, low throughput, operation of the process at a limited flow of the solutes, low efficiency, poor rejection power, particularly at low concentrations of the solute. Besides, membrane fouling is commonly caused by the accumulation of pollutants results in low separation efficiency and membrane flux in the long term [9-11]. Such disadvantages have prompted a growing interest in adsorption techniques because they can provide several advantages, such as easy operation, low cost, flexible operation, high removal effectiveness for a wide range of pollutants and problems [3].

Adsorption methods could be broadly divided into batch and flow-based procedures. The batch method is very simple and is an efficient tool for studying and determining the factors affecting the adsorption. In contrast, the batch technique is attractive to check the viability of the adsorbent to remove the water contaminants [2]. Various adsorbents have been studied for their adsorption performance toward dyes removal, which include activated carbon, graphene-based sorbents, biochar (BC), metal-organic frameworks, zeolites, biomaterials, nanoparticles, porous materials, clay minerals, and polymers [4]. Graphene-based sorbents include high carbon content, abundance of surface functional groups, special two-dimensional (2D) structure, superior physicochemical and mechanical properties, high surface area and pore volume, and numerous active sites [12-14]. Moreover, the presence of inorganic nanoparticles reduces the adsorbent aggregation and increases the efficiency of the adsorbents [15,16]. Pinky Yadav *et al.* [17] described the successful preparation of a rGO-ZnO nanocomposite by facile chemical precipitation method with an attempt to improve the visible light-induced photocatalytic degradation of brilliant green dye. The rGO-ZnO composite demonstrated superior photocatalytic performance, degrading 96.5% of the dye within 180 minutes under visible light, significantly outperforming pristine ZnO (41%). The composite exhibited excellent reusability, maintaining high efficiency over four cycles with minimal performance loss, and showed long-term storage stability. Afsaneh Padidar *et al.* [18] synthesized a highly efficient, magnetically separable graphite-based nanocomposite (Fe_3O_4/EG-chitosan) for the removal of Brilliant Green (BG) dye from aqueous solutions. Under optimal conditions - pH of 8.0, adsorbent dosage of 0.04 g, initial dye concentration of 50 ppm, and temperature of 293 K - the composite achieved a dye removal efficiency of 98%. The adsorption behavior followed the pseudo-second-order kinetic model and was best described by the Freundlich isotherm, indicating multilayer adsorption on a heterogeneous surface. Iftekhar Ahmad *et al.* [19]

developed an innovative Z-scheme ternary heterostructure, integrating graphene oxide (GO)-mediated polyaniline (PANI) with α-Fe_2O_3, and evaluated its photocatalytic performance under visible light for the degradation of Brilliant Green and ciprofloxacin. The composite demonstrated remarkable efficiency, achieving 99.8% degradation of Brilliant Green within 25 minutes and 93% degradation of ciprofloxacin within 90 minutes of light exposure. Compared to individual components, the degradation rate of Brilliant Green was 15 times higher than that of PANI and 10 times higher than α-Fe_2O_3, while ciprofloxacin degradation was enhanced by factors of 8.9 and 6.1, respectively. Qaiser Khan *et al.* [20] synthesized highly efficient TiO_2/reduced graphene oxide (TiO_2/rGO) nanocomposites using a simple hydrothermal method. By varying the rGO content to 0.5%, 1.0%, 2.0%, and 3.0%, while keeping the TiO_2 concentration constant, the resulting composites were labeled as TrG0.5, TrG1, TrG2, and TrG3, respectively. The photocatalytic performance of these composites was evaluated based on the degradation of Brilliant Green (BG) dye under UV light. Among the samples, TrG2 (containing 2% rGO) exhibited the highest degradation efficiency, with an apparent rate constant (kapp) of 0.023 min^{-1}, significantly outperforming pure TiO_2, which showed a kapp of only 0.006 min^{-1}. Rouhollah Khani *et al.* [21] developed a reduced graphene oxide/cobalt oxide (rGO/Co_3O_4) nanocomposite to serve as a selective, regenerable, and magnetically separable nanosorbent for the preconcentration and detection of Brilliant Green (BG) dye using UV-Vis spectrophotometry. Under optimized conditions, the system demonstrated a detection limit of 2.6 ng/mL, a relative standard deviation of 3.34% (n = 5), and an enrichment factor of 24.5, highlighting its sensitivity, precision, and potential for repeated use in dye analysis. Hou *et al.* [22] immobilized palladium–iron (Pd–Fe) magnetic nanoparticles onto reduced graphene oxide (rGO) to create an effective composite for the decolorization of toxic Brilliant Green dye in aqueous solutions. The adsorption process was found to be spontaneous and endothermic, following the pseudo-second-order kinetic model and best described by the Freundlich isotherm, indicating multilayer adsorption on a heterogeneous surface.

In the present study, BaFeO/GO-NCs have been synthesized and characterized by Fourier transform infrared (FTIR), X-ray diffraction (XRD), Field Emission Scanning Electron Microscopy (FESEM), Transmission Electron Microscopy (TEM), Vibrating Sample Magnetometer (VSM), and N_2 adsorption-desorption isotherm (Brunauer–Emmett–Teller (BET)). Additionally, the adsorption efficiency of the prepared BaFeO/GO-NCs to Brilliant Green Dye from aqueous solution have been tested by applying a set of batch experiments. The adsorption experiments were also evaluated under the influence of several parameters including pH, adsorbent dose, adsorbate concentration, and contact time. Moreover, the experimental data were authenticated by applying the adsorption kinetics and isotherm models.

2. Materials and Method

2.1 Chemicals

The following chemical reagents were purchased from Shanghai Chemical Reagent Co. Ltd: analytical-grade barium chloride dihydrate ($BaCl_2.2H_2O$, 99% BDH), ferric chloride hexahydrate ($FeCl_3.6H_2O$, 99% BDH), sodium hydroxide (NaOH), ammonium hydroxide (NH_4OH, 25%), potassium permanganate ($KMnO_4$, 99.9%), hydrogen peroxide (H_2O_2, 30%), sulfuric acid (H_2SO_4, 98%), hydrochloric acid (HCl, 37%), and nitric acid (HNO_3, 63%). However, brilliant green dye (BGD, $C_{27}H_{34}N_2O_4S$) used as model pollutant agents were obtained from (Merck, Germany).

2.2 Preparation of the Adsorbate (Brilliant Green Dye Solution)

Brilliant Green dye ($C_{27}H_{34}N_2O_4S$) (Merck, Germany) was bought from the market with molecular weight 482.62 g/mol and was used by dissolving 1 g of BG powder in 1 L of distilled water to prepare 1000 ppm of stock solution then diluted to other concentration through the experiment. The maximum wavelength was found to be 625 nm and the final concentrations were determined using UV-visible spectrophotometer (Varian Cary 300).

2.3 Synthesis of BaFeO/GO Nanocomposite

Pure GO nanosheets were synthesized from coal powder purchased from (Glentham Life Sciences) 40-60 micron 99.6% purity by the modified Hummers' method, (Tour's Method) [23] whereas BaFeO magnetic nanoparticles were synthesized by a modified co-precipitation method. The pure BaFeO nanoparticles and GO nanosheets were used for purposes of comparison with the BaFO/GO nanocomposites.

In a related approach, BaFeO/GO nanocomposites were prepared using a modified co-precipitation technique. Initially, $FeCl_3 \cdot 6H_2O$ and $BaCl_2 \cdot 2H_2O$ were dissolved in deionized water at a molar ratio of 2:1 (Fe:Ba). This solution was then combined with graphene oxide (GO) suspensions containing 10–30 wt% GO and stirred for 50 minutes. The resulting was continuously stirred and heated to 75 °C, then dropwise added 25 mL 0.75 M NaOH, the color is changed

immediately from orange to dark brown, which confirms the generation of BaFeO nanoparticles. The reaction mixture was stirred at 75 °C for another hour to complete the reaction. The obtained BaFeO/GO nanocomposite was further separated with the application of an external magnetic field and removed after 20 min of centrifugation to collect all particles. This product was then washed thoroughly for several times with deionized water and acetone to remove the impurities.

2.4 Characterization Techniques

The structural and physicochemical properties of the prepared samples were fully investigated by various analytical methods. XRD measurement: X-ray diffraction (XRD) measurements were taken on a PHILIPS PW1730 diffractometer (Netherlands) with Cu-Kα radiation, at room temperature with background signals corrected by linear interpolation. The functional groups of the samples were determined using Fourier transform infrared (FTIR) spectroscopy (Perkin Elmer TWO, USA); the spectra of samples were scanned in the range of 400 - 4000 cm^{-1}. For this, samples were mixed with potassium bromide (KBr), pressed into pellets, and analyzed accordingly. To evaluate surface characteristics, nitrogen adsorption–desorption isotherms were obtained at 77 K using a Quantachrome Autosorb - 61SA system, and the specific surface area was calculated using the Brunauer–Emmett–Teller (BET) method. Morphological features of the samples were examined through field-emission scanning electron microscopy (FESEM) using a TESCAN MIRA3 instrument, which provided detailed images of both surface and cross-sectional structures. Transmission electron microscopy (TEM) analysis, performed with a PHILIPS CM120 microscope, was used to observe nanoparticle distribution and morphology at the nanoscale, particularly highlighting the dispersion of BaFeO particles on GO nanosheets. Lastly, magnetic properties of the BaFeO/GO nanocomposites were assessed at room temperature using a vibrating sample magnetometer (VSM, MDKB), allowing for the recording of magnetization curves.

2.5 Brilliant Green Dye Adsorption Experiments

The adsorption of brilliant green dye experiments were carried out in a batch mode with a JAR test rotational speed of 200 rpm with 4 samples in one time as shown in Figure 1. Typically, 0.1 to 0.5 g of adsorbent material (BaFeO, BaFeO/10%GO, BaFeO/20%GO and BaFeO/30%GO) was added to 100 mL of a solution containing various amounts of the cationic brilliant green dye. UV-vis spectrophotometer was used to measure the brilliant green dye concentration at wavelength equals to 625 nm. In these experiments, the BG solution was initially set at a concentration of 75 mol/L with a pH of 7. The adsorption behavior of the samples (BaFeO, BaFeO with 10%, 20%, and 30% GO) was examined over different contact times ranging from 15 to 105 minutes. To investigate adsorption kinetics and the maximum adsorption capacity, BG solutions with concentrations between 75 and 150 ppm were prepared, maintaining a constant equilibration time of 30 minutes and a pH of 7. All adsorption measurements were carried out at room temperature (25 °C). The amount adsorbed (equation 1) and adsorption rate (percentage removal) (equation 2) were calculated from the difference in the pollutant concentration in the aqueous solution before and after adsorption according to the following equations:

$$q_e = \frac{(C_o - C_t) * V}{m} \quad (1)$$

$$\%\ Removal = \frac{(C_o - C_t)}{C_o} * 100\% \quad (2)$$

where, q_e is the amount of pollutants (mg/g) adsorbed on the adsorbent at equilibrium, C_0 and C_t (mg/L) are the initial pollutant concentration and the pollutant concentration at equilibrium, respectively, V (L) is the volume of the solution, and m (g) is the mass of the adsorbent.

BaFeO/GO-NCs have been synthesized and characterized by Fourier transform infrared (FTIR), X-ray diffraction (XRD), Field Emission Scanning Electron Microscopy (Fe-SEM), Transmission Electron Microscopy (TEM), Vibrating Sample Magnetometer (VSM), and N_2 adsorption-desorption isotherm (Brunauer–Emmett–Teller (BET)). Additionally, the adsorption efficiency of the prepared BaFeO/GO-NCs to Brilliant Green Dye from aqueous solution have been tested by applying a set of batch experiments. The adsorption experiments were also evaluated under the influence of several parameters including pH, adsorbent dose, adsorbate concentration, and contact time. Moreover, the experimental data were

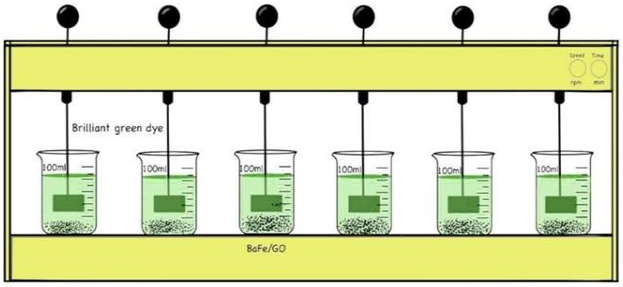

Figure 1. Schematic diagram of experimental setup.

authenticated by applying the adsorption kinetics and isotherm models.

3. Results and Discussion

3.1 FTIR Characterization

The chemical structure changes of the BaFeO-graphene oxide nanocomposite were investigated using Fourier-transform infrared spectroscopy (FTIR) in the wavenumber range of 450 – 4000 cm^{-1}, as shown in Figure 2. The FTIR spectra reveals characteristic bands associated with barium hexaferrite, hydroxyl (OH) groups, and graphene oxide. A prominent band at 609.95 cm^{-1} corresponds to the stretching vibrations of metal–oxygen bonds, confirming the formation of the hexaferrite structure involving both octahedral and tetrahedral coordination sites. The absorption band around 1619.29 cm^{-1} is attributed to the bending vibration of O–H bonds in water molecules that are chemically adsorbed on the surface of the magnetic particles. A broad band at approximately 3393.03 cm^{-1} indicates O–H stretching vibrations, reflecting both free and hydrogen-bonded hydroxyl groups. Additionally, O–H deformation vibrations appear at 1384.34 cm^{-1}. The bands observed at 2924.87 cm^{-1} and 2854.54 cm^{-1} correspond to C–H stretching vibrations. The peaks at 1110.26 cm^{-1} and 1194.28 cm^{-1} are assigned to C–O–C stretching vibrations, while the peak at 1075 cm^{-1} is due to C–O bond vibrations. Furthermore, the distinct peak at 1717.82 cm^{-1} is indicative of C=O (carbonyl) stretching, confirming the presence of graphene oxide functional groups in the composite [24-28].

3.2 SEM and TEM Characterizations

The surface morphology and internal structure of the synthesized BaFeO/GO nanocomposites were analyzed using Scanning Electron Microscopy (SEM) and Transmission Electron Microscopy (TEM), respectively. As illustrated in Figure 3a, the graphite powder was successfully oxidized to graphene oxide (GO). BaFeO nanoparticles, with a particle diameter of range 18 nm to 25 nm, were uniformly attached onto the GO sheets. TEM images in Figure 3b also reveal noticeable agglomeration of BaFeO nanoparticles within the GO matrix, attributed to the strong interactions between BaFeO and GO.

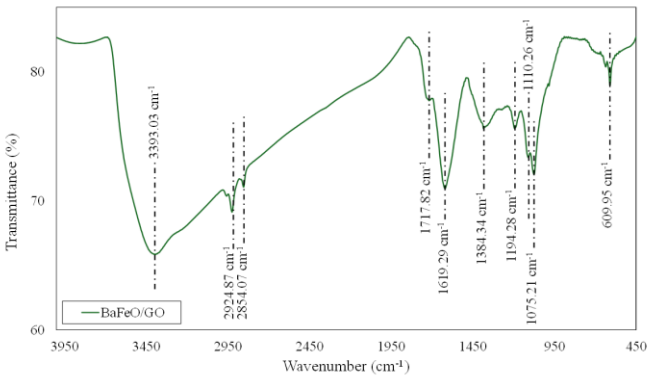

Figure 2. FTIR for the BaFeO/GO nanocomposites.

3.3 VSM Characterization

The magnetic properties of the synthesized Barium Ferrite/Graphene Oxide (BaFeO/GO) nanocomposites were analyzed using a vibrating-sample magnetometer (VSM) to assess their response to an external magnetic field as shown in Figure 4. The results revealed that the nanocomposites exhibited a saturation

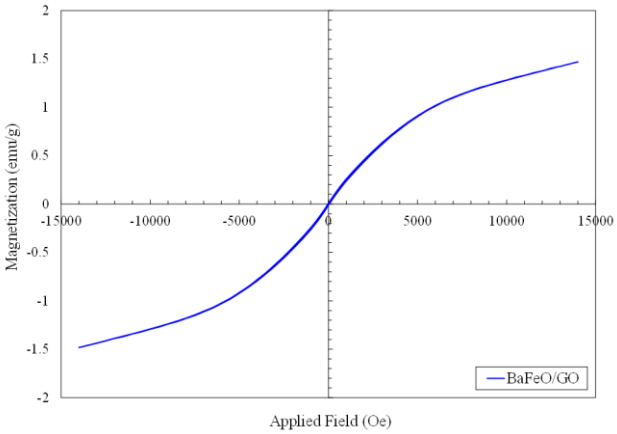

Figure 4. VSM for the synthesized BaFeO/GO nanocomposites.

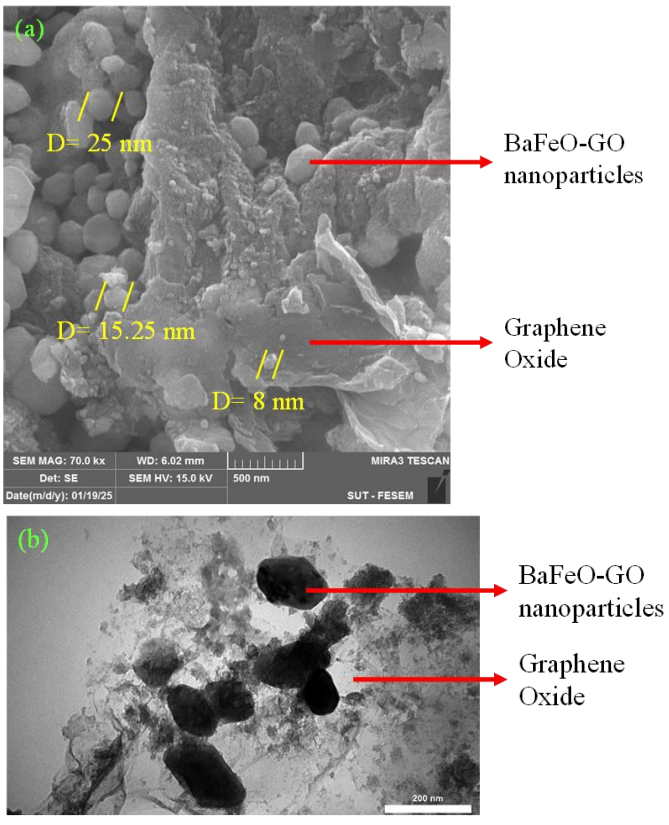

Figure 3. a) SEM images; b) TEM images.

magnetization (Ms) of 1.5 emu/g, indicating a relatively weak magnetic response. This limited magnetization is expected to influence the nanocomposites' performance in the removal of BG dye, as will be discussed in subsequent sections.

3.4 BET Surface Area and Pore Diameter Characterizations

The porosity of the synthesized BaFeO/GO nanocomposites was evaluated using nitrogen (N_2) adsorption–desorption isotherms and analyzed via the Brunauer–Emmett–Teller (BET) method. Figure 5 displays the N_2 adsorption–desorption isotherms for the BaFeO/GO nanocomposites. According to the IUPAC classification, the nanocomposites synthesized are of type IV. Based on the BET analysis, the specific surface area and pore volume were determined to be 73.74 m^2/g and 0.05 cm^3/g, respectively. Additionally, the average pore diameter, calculated using the Barrett–Joyner–Halenda (BJH) method, was found to be 2.7294 nm, indicating a nanoporous structure. A summary of these results is provided in Table 1 [23].

3.5 X-ray Diffraction Characterization

Figure 6 shows the XRD profiles of graphene oxide GO synthesized by Tour's method and BaFeO/GO nanocomposite. The high intensity peak was observed at 2θ = 9.6° of graphite oxide (GO), which corresponds to the (001) plane due to interlayer spacing caused by oxygen-containing functional groups. Upon co-precipitation with BaFeO, this peak often diminishes or disappears, indicating exfoliation or reduction of GO. This suggests that the BaFeO nanoparticles disrupt the regular stacking of GO layers, possibly due to intercalation or surface interactions. BaFeO has a well-defined hexagonal crystal structure, leading to distinct diffraction peaks at specific 2θ angles, such as approximately 27.08°, 28.9°, 31.78°, 33.1°, and 42.9°, corresponding to planes like (108), (113), (204), and (205). The appearance of these peaks in the composite's XRD pattern confirms the successful formation of crystalline BaFeO within the GO matrix [29].

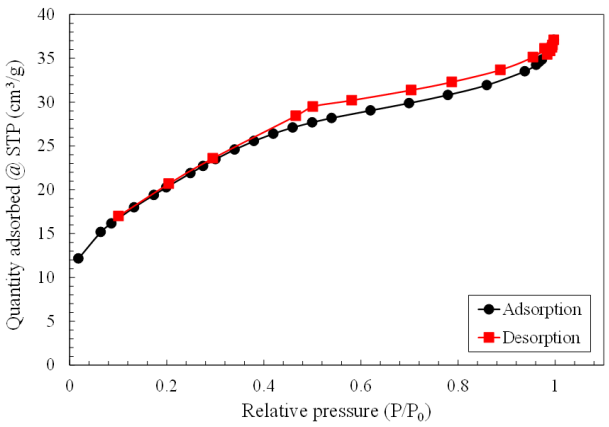

Figure 5. N_2 adsorption–desorption isotherms for the BaFeO/GO nanocomposites.

3.6 Effect of Adsorbent Dosage

Figure 7 illustrates the effect of adsorbent dosage (0.1, 0.2, 0.3, 0.4, and 0.5 g) on the removal efficiency of brilliant green dye (75 ppm) after 30 minutes of contact time. An increase in the graphene oxide (GO) content from 0% to 30% in the BaFeO/GO nanocomposites led to a significant enhancement in dye removal. This improvement is attributed to the increased number of active adsorption sites and the larger specific surface area provided by GO. At the highest adsorbent dosage (0.5 g), nanocomposites containing 30% GO achieved a removal efficiency of 98.9%, compared to 67.8% for those without GO. This substantial difference highlights the critical role of GO in enhancing the adsorption of brilliant green dye.

3.7 Effect of Initial Dye Concentration

The influence of initial brilliant green (BG) dye concentration (75, 100, 125, and 150 ppm) on the percentage removal of dye after 30 minutes of contact time is presented in Figure 8. A decrease in removal percentage was observed with increasing initial dye concentration. This trend

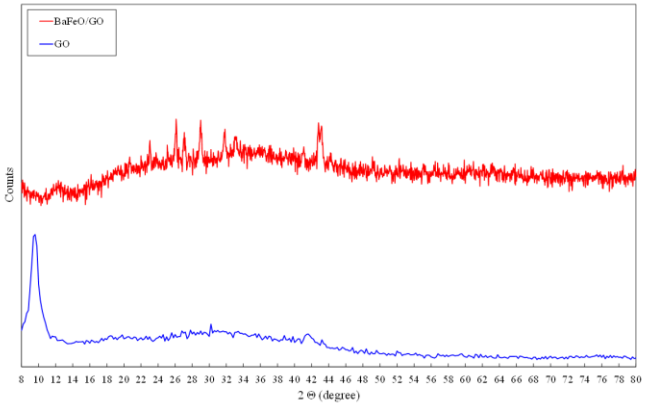

Figure 6. XRD pattern for the graphene oxide (GO) and the nanocomposites (BaFeO/GO).

Table 1. N_2 adsorption–desorption isotherms for the BaFeO/GO nanocomposites.

Sample	BET surface area (m^2/g)	Pore volume (cm^3/g)	Average pore diameter (nm)
BaFeO/Go	73.7449	0.053667	2.7294

can be attributed to the greater availability of active adsorption sites at lower dye concentrations, allowing more dye molecules to be captured by the nanocomposite surface. In contrast, at higher concentrations, the limited number of available binding sites becomes saturated, reducing the likelihood of dye adsorption and resulting in a lower removal efficiency.

3.8 Effect of Contact Time

Figure 9 shows the influence of contact time on the removal efficiency of 75 ppm brilliant green (BG) dye using nanocomposites of varying compositions. The dye removal percentage increased steadily and reached near-equilibrium within approximately 60 minutes. Extending the contact time to 105 minutes resulted in only a marginal increase (~2.5%) in removal efficiency, indicating that prolonged contact beyond 60 minutes offers limited benefit. This plateau effect is likely due to the aggregation of dye molecules over time, which hinders their diffusion into the deeper, high-energy adsorption sites within the adsorbent. As these nanopores become saturated, further adsorption is impeded. Given the minimal change in removal efficiency between 60 mins and 105 mins, the system was considered to have reached a quasi-equilibrium after 60 minutes, and a steady-state approximation was applied [30].

3.9 Effect of pH

The pH parameter was investigated within the range (2-12) at 75 ppm for different nanocomposites compositions for 30 mins contact time as shown in Figure 10. The pH plays a vital role in the adsorption process by affecting the surface charge of the nanocomposites, the ionization state of the BG dye molecules, the dissociation behavior of functional groups on the adsorbent's active sites, and the overall structure of the dye. The results indicate that dye removal efficiency increases with pH, reaching a maximum at pH of 7, and then declines as pH continues to rise to 12. At lower pH values, the surface of the adsorbent becomes protonated due to excess H^+ ions, leading to electrostatic repulsion with the cationic BG dye, thereby reducing adsorption efficiency. Conversely, at pH levels above 7, the decrease in removal efficiency is likely attributed

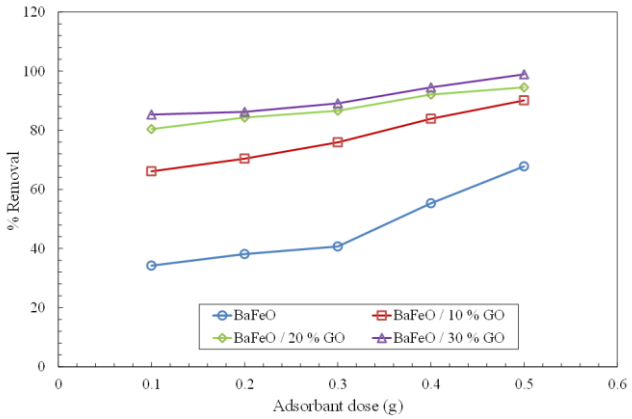

Figure 7. Effect of absorbent dosage on percentage removal of brilliant green.

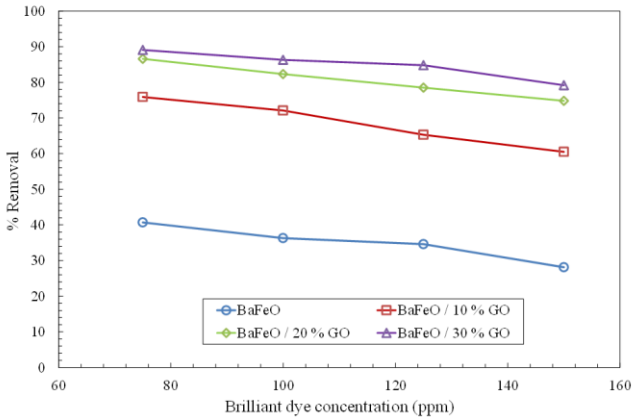

Figure 8. Effect of initial dye concentration on percentage removal.

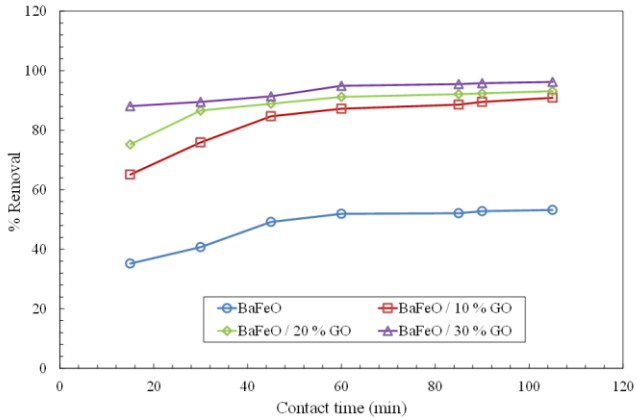

Figure 9. Effect of contact time on percentage removal.

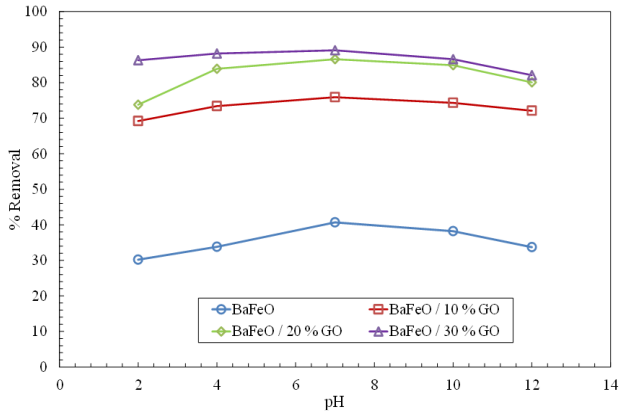

Figure 10. Effect of pH on percentage removal.

to competition for active adsorption sites and possible changes in the adsorbent's surface chemistry [31-33].

3.10 Adsorption Kinetic Study

In order to investigate the adsorption of BG onto the BaFeO/GO nanocomposites, pseudo-first order (equation 3), pseudo-second order (equation 4) were used [34].

$$\log (q_e - q_t) = \log(q_e) - k_1 t \quad (3)$$

$$\frac{t}{q_t} = \frac{1}{k_2 q_e^2} + \frac{t}{q_e} \quad (4)$$

Where, q_t is the amount of adsorbate adsorbed at time t (mg/g), q_e is the adsorption capacity at equilibrium (mg/g), k_1 is the pseudo-first-order rate constant (1/min), and t is the contact time (min), and k_2 is the pseudo-second-order rate constant (mg/(g.min)). The kinetic rate constant, k, and q_e for each model can be calculated by plotting graph log (q_e-q_t) versus t for pseudo-first order, t/q_t versus t for pseudo-second-order models. All the kinetic parameters for all kinetics models were calculated from the graph and presented in Table 2. As shown in Figures 11 and 12, the correlation factor (R^2) obtained calculated through pseudo-second- order models (R^2 = 0.9997) greater than pseudo-first order (R^2 = 0.9664), this implies that the experimental data were good agreement with pseudo-second kinetics order model.

3.11 Adsorption Equilibrium Isotherm

Adsorption isotherms are important for the study of an adsorbate with an adsorbent. They offer valuable information in to the mechanism and strength of the adsorption process, such as how the molecules partition between the solid-liquid phases at equilibrium. These representations are useful for assessing the performance and optimal usage of different adsorbents. The isotherm curves, in particular, explain the mechanism of the adsorption process and provide important information on the maximum adsorption capacity of the adsorbent material. Equilibrium data were applied to the Langmuir and Freundlich isotherms from literature to determine the most suitable isotherm model. These models are widely used to characterize the adsorption processes on account of the variation susceptibility towards the adsorption behaviors and surface properties. The Langmuir isotherm (Equation 5) is for a monolayer adsorption on a surface with a finite number of identical, energetically equivalent sites and suggests uniform surface. On the other hand, the Freundlich isotherm (Equation 6) is an empirical model which considers the adsorption in

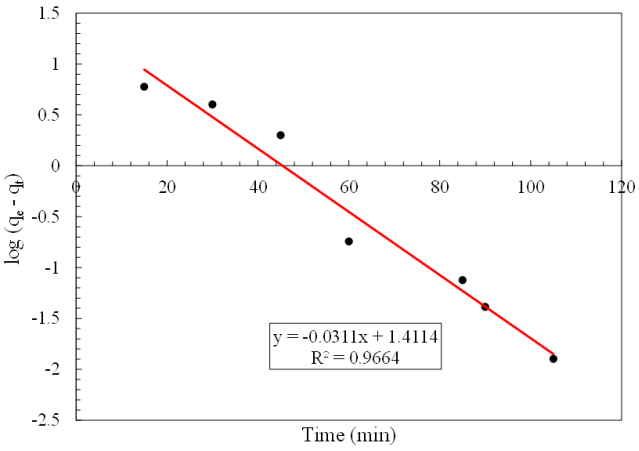

Figure 11. Pseudo-first order model at different contact time (15-105 min), BG dye concentration 75 ppm, and nanocomposite composition (BaFeO/30%GO).

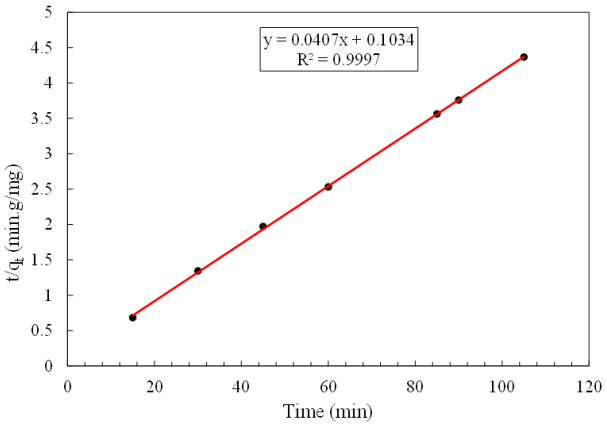

Figure 12. Pseudo-second order model at different contact time (15-105 min), BG dye concentration 75 ppm, and nanocomposite composition (BaFeO/30%GO).

Table 2. Kinetic parameters for Pseudo-first order and Pseudo-second order models.

Kinetics model	q_e (experimental) (mg/g)	q_e (calculated) (mg/g)	R^2	Rate constant (k)
Pseudo-first order	24	24.02	0.9664	-0.0311 s^{-1}
Pseudo-second order	24	24.57	0.9997	0.01602 $\frac{mg}{g.min}$

a heterogeneous surface with adsorption sites of different energy, resulting in a nonuniform distribution of adsorption heat [34].

$$\frac{C_e}{q_e} = \frac{1}{bq_m} + \frac{C_e}{q_m} \quad (5)$$

$$\log(q_e) = \log(k_f) - \frac{\log(C_e)}{n} \quad (6)$$

Where C_e is the equilibrium concentration of the solute in the solution (mmol/L), q_e is the amount of solute adsorbed per unit mass of adsorbent at equilibrium (mmol/g), q_m is the maximum adsorption capacity corresponding to complete monolayer coverage (mmol/g), and b is the Langmuir constant (L/mmol), which relates to the affinity between the adsorbate and the adsorbent. k_f is the Freundlich constant indicative of adsorption capacity, and n is a constant that indicates the adsorption intensity or surface heterogeneity.

To assess which model best fits the experimental data, isotherm curves were plotted. For the Langmuir model (Figure 13), a linear plot of C_e/q_e versus C_e was used, while the Freundlich model (Figure 14) was evaluated using a log–log plot of log (q_e) versus log (C_e). From the Langmuir plot, the slope and intercept provide the values of q_m and b, allowing the determination of the monolayer adsorption capacity and the nature of the adsorption interaction. Similarly, the Freundlich constants k_f and n were derived from the intercept and slope of the log-transformed plot. The calculated isotherm parameters along with the correlation coefficients (R^2) for both models are summarized in Table 3. As observed, the Langmuir model shows a high correlation coefficient ($R^2 = 0.9997$), indicating an excellent fit to the experimental data. This suggests that the adsorption process is more accurately described by the Langmuir isotherm, supporting the assumption of monolayer adsorption behavior in the aqueous system.

4. Conclusion

This study successfully synthesized barium ferrite/graphene oxide (BaFeO/GO) nanocomposites using a modified co-precipitation method and evaluated their potential as adsorbents for brilliant green dye (BGD) removal from aqueous media. Structural and surface analyses confirmed the effective incorporation of GO, which enhanced surface area, pore structure, and functional groups, leading to improved dye–adsorbent interactions. Batch adsorption experiments demonstrated that BaFeO/GO nanocomposites, particularly at 30 wt% GO, exhibited high removal efficiency under optimal conditions, achieving up to 98.9% dye removal. Kinetic and isotherm studies indicated that the adsorption process is chemisorption-driven and best described by the Langmuir model, confirming monolayer adsorption on a homogeneous surface. Overall, the findings establish BaFeO/GO nanocomposites as effective and promising adsorbents for dye removal applications.

Acknowledgment

This research work was not funded by any organization.

Table 3. Adsorption isotherms parameters.

Isotherm model	Model parameters	R^2
Langmuir model	q_m= 21.28 ; b = -2.714	0.9997
Freundlich	k_f =1.627 ; n = 0.077	0.9854

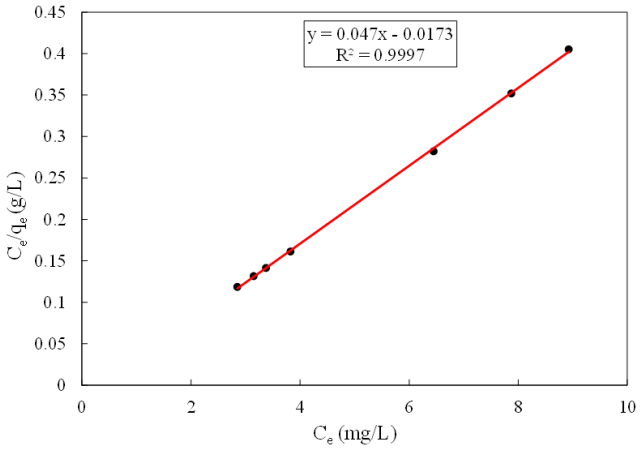

Figure 13. Langmuir isotherm model at different contact time (15-105 min), BG dye concentration 75 ppm, and nanocomposite composition (BaFeO/30%GO).

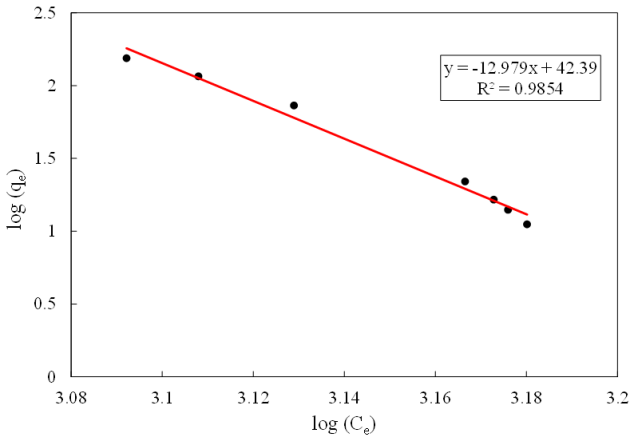

Figure 14. Freundlich isotherm model at different contact time (15-105 min), BG dye concentration 75 ppm, and nanocomposite composition (BaFeO/30%GO).

CRedit Author Statement

Author Contributions: Usama A. Saed: Conceptualization, Methodology, Investigation, Resources, and Data Curation, Writing, Supervision; Alaa H. Ali: Conceptualization, Methodology, Formal Analysis, Data Curation; Ammar A. Saoud: Validation, Data Curation; Zeyad Zeitoun: Writing, Review and Editing, Supervision. All authors have read and agreed to the published version of the manuscript.

References

[1] Gregory, P. (2000) Dyes and dye intermediates. *Kirk-Othmer Encyclopedia of Chemical Technology*, p. 1-66. DOI: 10.1002/0471238961.0425051907180507.a01.pub2.

[2] Dave, S., Das, J., Varshney, B., Sharma, V.P. (2022) Dyes and pigments: Interventions and how safe and sustainable are colors of life, in *Trends and Contemporary Technologies for Photocatalytic Degradation of Dyes*. Springer. p. 1-20. DOI: 10.1007/978-3-031-08991-6_1.

[3] Mansour, R.A.E.-G., Simeda, M.G., Zaatout, A.A. (2021) Removal of brilliant green dye from synthetic wastewater under batch mode using chemically activated date pit carbon. *RSC Advances*, 11(14), 7851-7861. DOI: 10.1039/D0RA08488C.

[4] Aqeel, K., Mubarak, H.A., Amoako-Attah, J., Abdul-Rahaim, L.A., Al Khaddar, R., Abdellatif, M., Al-Janabi, A., Hashim, K.S. (2020) Electrochemical removal of brilliant green dye from wastewater. *IOP Conference Series: Materials Science and Engineering*. IOP Publishing. DOI: 10.1088/1757-899X/888/1/012036.

[5] Booton, A., Mayer, B.K., Zitomer, D.H. (2024) Chemical oxidation as an alternative for municipal wastewater secondary treatment: a review. *Reviews in Environmental Science and Bio/Technology*, 23(1), 43-65. DOI: 10.1007/s11157-024-09684-5.

[6] Farsang, E., Horváth, K., Beck, A., Wang, Q., Lauber, M., Guillarme, D., Fekete, S. (2020) Impact of the column on effluent pH in cation exchange pH gradient chromatography, a practical study. *Journal of Chromatography A*, 1626, 461350. DOI: 10.1016/j.chroma.2020.461350.

[7] Rane, A., Joshi, S.J. (2021) Biodecolorization and biodegradation of dyes: A review. *The Open Biotechnology Journal*, 15(1), 97-108. DOI: 10.2174/1874070702115010097.

[8] Guo, S., Wang, H., Liu, X., Zhang, Z., Liu, Y. (2024) Approaches for the treatment and resource utilization of electroplating sludge. *Materials*, 17(7), 1707. DOI: 10.3390/ma17071707.

[9] Zeitoun, Z., El-Shazly, A., Sameh, M., Ragab, M., Nosier, S., Moharram, M. (2021) Electrospinning of polyvinylidene fluoride membranes: Effect of membrane composition and fabrication conditions. *Egyptian Journal of Chemistry*, 65, 41-50. DOI: 10.21608/ejchem.2021.77967.3913.

[10] Zeitoun, Z., El-Shazly, A.H., Nosier, S., Elmarghany, M.R., Salem, M.S., Taha, M.M. (2020) Performance Evaluation and Kinetic Analysis of Photocatalytic Membrane Reactor in Wastewater Treatment. *Membranes*, 10(10), 276. DOI: 10.3390/membranes10100276.

[11] Zeitoun, Z., Selem, N.Y. (2023) A comprehensive review on textile wastewater treatment by coupling TiO2 with PVDF membrane. *Bulletin of the National Research Centre*, 47(1), 153. DOI: 10.1186/s42269-023-01131-9.

[12] Ani, P.C., Al-Abedi, H.J., Smith, J.D., Zeitoun, Z. (2025) Comparative Morphological and Thermal Analysis of Biochar from Oak, and from Oak, Pine and RDF Blends, in a Downdraft Gasifier. *Fuels*, 6(3). 73. DOI: 10.3390/fuels6030073.

[13] Ani, P.C., Alhameedi, H., Al-Abedi, H.J., Al-Rubaye, H., Zeitoun, Z., Ewuzie, U., Smith, J.D. (2025) The Comprehensive Quantification and Characterization of Oak Biochar Produced via a Gasification Process Using a Downdraft Reactor. *Fuels*, 6(3), 51. DOI: 10.3390/fuels6030051.

[14] Ani, P.C., Al-Abedi, H.J., Smith, J.D., Zeitoun, Z. (2025) Biochar Surface Chemistry Modification by Blending Hardwood, Softwood, and Refuse-Derived Fuel: Insights from XPS, FTIR, and Zeta Potential Analysis. *Fuels*, 6(3), 71. DOI: 10.3390/fuels6030071.

[15] Kyzas, G.Z., Deliyanni, E.A., Matis, K.A. (2014) Graphene oxide and its application as an adsorbent for wastewater treatment. *Journal of Chemical Technology & Biotechnology*, 89(2), 196-205. DOI: 10.1002/jctb.4220.

[16] Ramesha, G., Kumara, A.V., Muralidhara, H., Sampath, S. (2011) Graphene and graphene oxide as effective adsorbents toward anionic and cationic dyes. *Journal of Colloid and Interface Science*, 361(1), 270-277. DOI: 10.1016/j.jcis.2011.05.050.

[17] Yadav, P., Kapil, I., Dutta, M., Bhaduri, A. (2024) Effectual visible-driven photocatalytic performances on brilliant green dye by reduced graphene oxide–zinc oxide nanocomposite. *Ionics*, 30(5), 2927-2937. DOI: 10.1007/s11581-024-05450-3.

[18] Padidar, A., Mohammadi, A. (2024) Development of a magnetite nanocomposite based on expanded graphite/chitosan for efficient removal of brilliant green dye from aqueous solutions. *Separation Science and Technology*, 59(6-9), 954-966. DOI: 10.1080/01496395.2024.2358206.

[19] Ahmad, I., Athar, M.S., Muneer, M., Altass, H.M., Felemban, R., Ahmed, S.A. (2025) Synergistic design of a graphene oxide-mediated polyaniline/α-Fe2O3 ternary heterostructure: advancing photocatalytic degradation and adsorption efficiency. *Nanoscale*, 17(7), 3822-3836. DOI: 10.1039/D4NR03681F.

[20] Khan, Q., Sayed, M., Gul, I. (2023) Titania/reduced graphene oxide nanocomposites (TiO2/rGO) as an efficient photocatalyst for the effective degradation of brilliant green in aqueous media: effect of peroxymonosulfate and operational parameters. *Environmental Science and Pollution Research*, 30(27), 71025-71047. DOI: 10.1007/s11356-023-27316-3.

[21] Khani, R., Irani, M. (2020) A reusable reduced graphene oxide-cobalt oxide nanocomposite with excellent yield as adsorbent for determination trace-level of brilliant green in environmental water samples. *Research on Chemical Intermediates*, 46(4), 2137-2154. DOI: 10.1007/s11164-020-04083-1.

[22] Hou, Y., Qi, J., Hu, J., Ruan, W., Xiang, Y., Wei, X. (2022) Decolorizing brilliant green by mesoporous Pd–Fe magnetic nanoparticles immobilized on reduced graphene oxide: Artificial neural network modeling. *International Journal of Environmental Science and Technology*, 19(5), 3935-3946. DOI: 10.1007/s13762-021-03283-5.

[23] Bukovska, H., García-Perez, F., Brea Núñez, N., Bonales, L.J., Velasco, A., Clavero, M.Á., Martínez, J., Quejido, A.J., Rucandio, I., Gómez-Mancebo, M.B. (2023) Evaluation and Optimization of Tour Method for Synthesis of Graphite Oxide with High Specific Surface Area. *Journal of Carbon Research*, 9(3), 65. DOI: 10.3390/c9030065.

[24] Rani, S., Kumar, M., Garg, R., Sharma, S., Kumar, D. (2016) Amide functionalized graphene oxide thin films for hydrogen sulfide gas sensing applications. *IEEE Sensors Journal*, 16(9), 2929-2934. DOI: 10.1109/JSEN.2016.2524204.

[25] Bae, H., Ahmad, T., Rhee, I., Chang, Y., Jin, S.-U., Hong, S. (2012) Carbon-coated iron oxide nanoparticles as contrast agents in magnetic resonance imaging. *Nanoscale Research Letters*, 7, 1-5. DOI: 10.1186/1556-276X-7-44.

[26] Sayed, A., Fayed, M.S., Kassem, M., Ezz, T. (2011) Different Factors Affecting the Preparation of Hexagonal Barium Ferrite and its Evaluation by Radar Wave Absorption. in International Conference on Aerospace Sciences and Aviation Technology. *International Conference on Aerospace Sciences and Aviation Technology*, 14, 1-7. DOI: 10.21608/asat.2011.23276.

[27] Hojjati Najafabadi, A., Ghasemi, A., Mozaffarinia, R. (2016) Synthesis and evaluation of microstructural and magnetic properties of Cr3+ substitution barium hexaferrite nanoparticles (BaFe10.5−xAl1.5CrxO19). *Journal of Cluster Science*, 27, 965-978. DOI: 10.1007/s10876-015-0963-x.

[28] Goel, S., Garg, A., Gupta, R.K., Dubey, A., Prasad, N.E., Tyagi, S. (2020) Development of RGO/BaFe12O19-based composite medium for improved microwave absorption applications. *Applied Physics A*, 126(6), 436. DOI: 10.1007/s00339-020-03613-3.

[29] Maddahfar, M., Ramezani, M., Mostafa Hosseinpour-Mashkani, S. (2016) Barium hexaferrite/graphene oxide: controlled synthesis and characterization and investigation of its magnetic properties. *Applied Physics A*, 122, 1-9. DOI: 10.1007/s00339-016-0283-5.

[30] Mane, V.S., Mall, I.D., Srivastava, V.C. (2007) Kinetic and equilibrium isotherm studies for the adsorptive removal of Brilliant Green dye from aqueous solution by rice husk ash. *Journal of Environmental Management*, 84(4), 390-400.

[31] Abate, G.Y., Alene, A.N., Habte, A.T., Getahun, D.M. (2020) Adsorptive removal of malachite green dye from aqueous solution onto activated carbon of Catha edulis stem as a low cost bio-adsorbent. *Environmental Systems Research*, 9, 1-13. DOI: 10.1186/s40068-020-00191-4.

[32] Ai, L., Zhang, C., Liao, F., Wang, Y., Li, M., Meng, L., Jiang, J. (2011) Removal of methylene blue from aqueous solution with magnetite loaded multi-wall carbon nanotube: kinetic, isotherm and mechanism analysis. *Journal of Hazardous Materials*, 198, 282-290. DOI: 10.1016/j.jhazmat.2011.10.041.

[33] Bello, O.S., Adegoke, K.A., Akinyunni, O.O. (2017) Preparation and characterization of a novel adsorbent from Moringa oleifera leaf. *Applied Water Science*, 7, 1295-1305. DOI: 10.1007/s13201-015-0345-4.

[34] Abate, G.Y., Alene, A.N., Habte, A.T., Getahun, D.M. (2020) Adsorptive removal of malachite green dye from aqueous solution onto activated carbon of Catha edulis stem as a low cost bio-adsorbent. *Environmental Systems Research*, 9(1), 29. DOI: 10.1186/s40068-020-00191-4.